Investigation of the Excited-State Electron Transfer and Cage-Escape Yields Between Halides and a Fe(III) Photosensitizer

Simon De Kreijger,[‡] Alexia Ripak,[‡] Benjamin Elias[‡]* and Ludovic Troian-Gautier[‡,ϕ]*

[‡] UCLouvain, Institut de la Matière Condensée et des Nanosciences (IMCN), Molecular Chemistry, Materials and Catalysis (MOST), Place Louis Pasteur 1/L4.01.02, B-1348 Louvain-la-Neuve, Belgium

[ϕ] Wel Research Institute, Avenue Pasteur 6, 1300 Wavre, Belgium

KEYWORDS. Cage-Escape Yields • Iron • Halide • Oxidation • Earth Abundant

ABSTRACT: Excited-state quenching and reduction of $[Fe(phtmeimb)_2]^+$, where phtmeimb is phenyl[tris(3-methyl-imidazolin-2-ylidene)]borate, with iodide, bromide and chloride were studied in dichloromethane, acetonitrile, and acetonitrile/water 1:1 mixture by means of steady-state and time-resolved spectroscopic techniques. Quenching rate constants were almost diffusion-limited in dichloromethane and acetonitrile and followed the expected periodic trend, i.e. I^->Br^->Cl^-. Confirmation of excited-state reductive electron transfer was only unambiguously obtained when iodide was used as quencher. The cage-escape yields, i.e. the separation of the geminate radical pair formed upon bimolecular excited-state electron transfer were determined. These yields were larger in dichloromethane (0.079) than in acetonitrile (0.017) and no photoproduct could be observed in acetonitrile/water 1:1. This study further emphasizes that solvents with low dielectric constant are more suited for productive excited-state electron transfer using Fe(III) photosensitizers with ^{2}LMCT excited-state.

The current energy landscape requires new approaches to solar fuels formation. Solar energy has long been considered a prime alternative with several technologies that have been developed over the years.[1-16] Solar energy conversion to electricity is commonly efficiently achieved with photovoltaic panels. Yet, a dichotomy exists between the moment when energy is most needed and when sunlight reaching the earth is the most intense. Hence, current developments are focused on novel avenues to store solar energy. Batteries are an obvious choice that presents several benefits but also some limitations.[17] An alternative is to store solar energy in chemical bonds, i.e. the so-called *solar fuels*.[1, 18-26] Typical examples include hydrogen gas (H_2) which is considered worldwide as a promising target for large scale energy storage and distribution.[27] Alternative solar fuels include liquid fuels from CO_2 reduction,[8, 28-29] as well as halogen (X_2), that could be concomitantly formed with H_2 upon hydrohalic acid (HX) splitting.[30-31] HX splitting would operate according to a mechanism depicted in **Figure 1** where the excited photosensitizer oxidizes the halide (X^-), forming the corresponding $X^{\bullet}$ that further reacts with X^- to form $X_2^{\bullet-}$. The reduced photosensitizer can activate a proton reduction catalyst that in turn generates H_2 from a proton source. The main drawback of hydrohalic splitting is the thermodynamic demand associated with halide oxidation. Aqueous halide oxidation occurs at potentials $E°(X^{\bullet/-})$ of 1.33, 1.93 and ~2.1-2.3V vs NHE for iodide, bromide and chloride, respectively.[23] This wide range of potentials was shown to be narrower in organic solvents where $E°(X^{\bullet/-})$ of 1.23, 1.35 and 1.46 V vs NHE have been roughly estimated in acetonitrile for iodide, bromide and chloride, respectively.[32-33] Hence, such oxidations are thermodynamically very demanding in water and often requires using photosensitizers based on rare ruthenium and iridium metals. Whereas evidence for iodide or bromide oxidation in organic solvent with Ru(II) and Ir(III) photosensitizers was unambiguously confirmed by transient absorption spectroscopy,[32-34] it is only very recently that evidence for chloride oxidation in water-like conditions was provided using Ir(III) dinuclear photosensitizers.[34] Notably bromide and chloride photo-oxidation have been monitored in acetone using Ru(II) photosensitizers[35-37] as well as by one- or two-photon excitation of N-phenylphenothiazine in acetonitrile.[38]

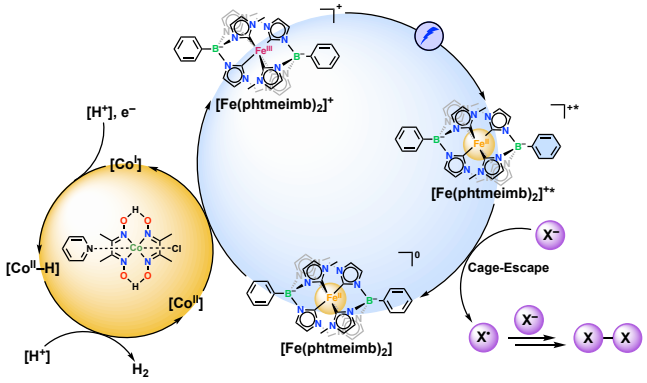

Figure 1. Structure of $[Fe(phtmeimb)_2]^+$ alongside the proposed scheme for the HX (X = I, Br, Cl) splitting reaction. The mechanism for hydrogen production using $[Fe(phtmeimb)_2]^+$ has been proposed by Wärnmark and co-workers.[39] Halide oxidation represents the focus of this work.

The use of Ir(III) and Ru(II) photosensitizers helps perform these challenging oxidations using single photon excitation but represents a drawback in terms of sustainability. A luminescent iron(III) photosensitizer $[Fe(phtmeimb)_2]^+$ (**Figure 1**), where phtmeimb is phenyl[tris(3-methyl-imidazolin-2-

ylidene)]borate, was recently pioneered by Wärnmark and coworkers.[40] This photosensitizer has been thoroughly characterized spectroscopically and its use in photoredox catalysis and hydrogen photoproduction has also been documented,[39-49] but it has yet to be used for halide oxidation, which could open the way to HX splitting. With its 2 ns excited-state lifetime and excited-state reduction and oxidation potential of 1.6 V and –1.3 V vs NHE respectively, this photosensitizer shows great promise for excited-state electron transfer and catalysis.[40] In here, we investigated the use of $[Fe(phtmeimb)_2]^+$ as photosensitizer for halide oxidation in dichloromethane (CH_2Cl_2), acetonitrile (CH_3CN) and CH_3CN/H_2O 1:1 mixture. In neat organic solvent, large quenching rate constant close to the diffusion limit were obtained. In CH_3CN/H_2O 1:1 mixture, iodide and to a lesser extend bromide were competent for excited-state quenching. Direct evidence for excited-state electron transfer was only obtained by nanosecond transient absorption spectroscopy for iodide in dichloromethane and acetonitrile. The cage-escape yields were also determined and were shown to be larger in dichloromethane (0.079) than in acetonitrile (0.017). Altogether, the results presented herein represent a first step towards the transition to earth abundant photosensitizers for halide oxidation, albeit only in organic solvent.

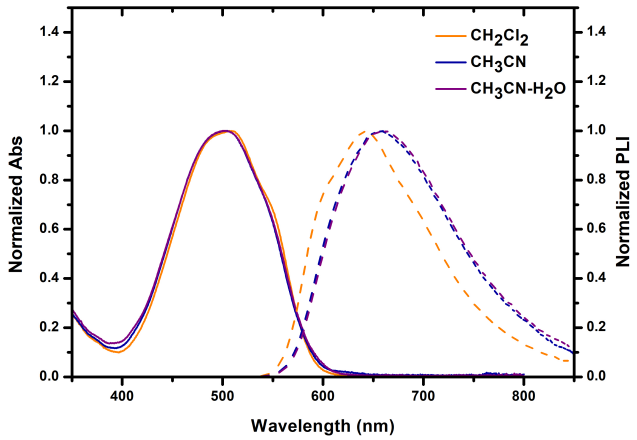

Figure 2. UV-Vis (solid lines) and photoluminescence (dashed lines) spectra of $[Fe(phtmeimb)_2]^+$ recorded at room temperature under air in CH_2Cl_2 (orange), CH_3CN (blue) and CH_3CN/H_2O 1:1 (purple).

The ground-state absorption and excited-state photoluminescence spectra (**Figure 2**) were only slightly sensitive to the solvent nature, as expected for the doublet ligand-to-metal charge transfer excited-state character of $[Fe(phtmeimb)_2]^+$.[40, 45] The excited-state lifetime was also not drastically affected and ranged from 1.8 ns in CH_3CN/H_2O 1:1 to 2.4 ns in CH_2Cl_2.

Excited-state quenching was then investigated with tetra-*n*-butylammonium iodide, bromide and chloride in CH_2Cl_2, CH_3CN and CH_3CN/H_2O 1:1 mixture (**Figure 3** and **Figures S1-S12**). In CH_3CN, the quenching rate constants (k_q) followed the expected periodic trend with k_q that ranged from 1.49 x10^{10} to 2.06 x10^{10} $M^{-1}s^{-1}$ for chloride and iodide, respectively (**Table 1**).[50]

Table 1. Excited-state quenching rate constants for the reaction between $[Fe(phtmeimb)_2]^+$ and tetra-*n*-butylammonium halide.

Solvent	k_q (x10^{10} $M^{-1}s^{-1}$)		
	Iodide	Bromide	Chloride
CH_3CN	2.06	1.87	1.49
CH_3CN:H_2O 1:1	1.46	0.25	---[d]
CH_2Cl_2	2.03	2.02	1.71
CH_2Cl_2[a]	2.14	2.05	1.63
CH_2Cl_2[b]	0.39	0.31	0.24
CH_2Cl_2[c]	0.39	0.30	0.20

[a]eluted through basic Al_2O_3. [b]with 0.5 M $TBAPF_6$. [c]eluted through basic Al_2O_3 and with 0.5 M $TBAPF_6$. [d]no excited-state quenching observed.

The k_q in CH_3CN/H_2O 1:1 slightly decreased to values of 1.46 x10^{10} and 2.49 x10^9 $M^{-1}s^{-1}$ for iodide and bromide, respectively. Excited-state quenching with chloride could not be observed under these conditions. In dichloromethane, the k_q were on the same order of magnitude as those determined in acetonitrile (**Table 1**). Note that, in neat dichloromethane, the downward curvature of the Stern-Volmer plots at higher quencher concentrations was most likely due to the kinetic salt effect and the quenching rate constants with chloride in neat dichloromethane are an estimate.[51-56] The excited-state quenching experiments were thus performed in dichloromethane containing 0.5 M of tetra-*n*-butylammonium hexafluorophosphate ($TBAPF_6$). A ~10 fold excess of $TBAPF_6$ *vs* halide in neat CH_2Cl_2 was used to investigate this kinetic salt effect. In this case, the excited-state quenching rate constant were one order of magnitude smaller, i.e. 3.9 x10^9, 3.1 x10^9 and 2.4 x10^9 $M^{-1}s^{-1}$ for iodide, bromide and chloride, respectively. This is in line with a decreased diffusion rate upon the introduction of large concentration of electrolyte. All experiments were also repeated with dichloromethane freshly eluted over basic Al_2O_3 to remove any residual traces of HCl or other impurities, which led to identical results.[57]

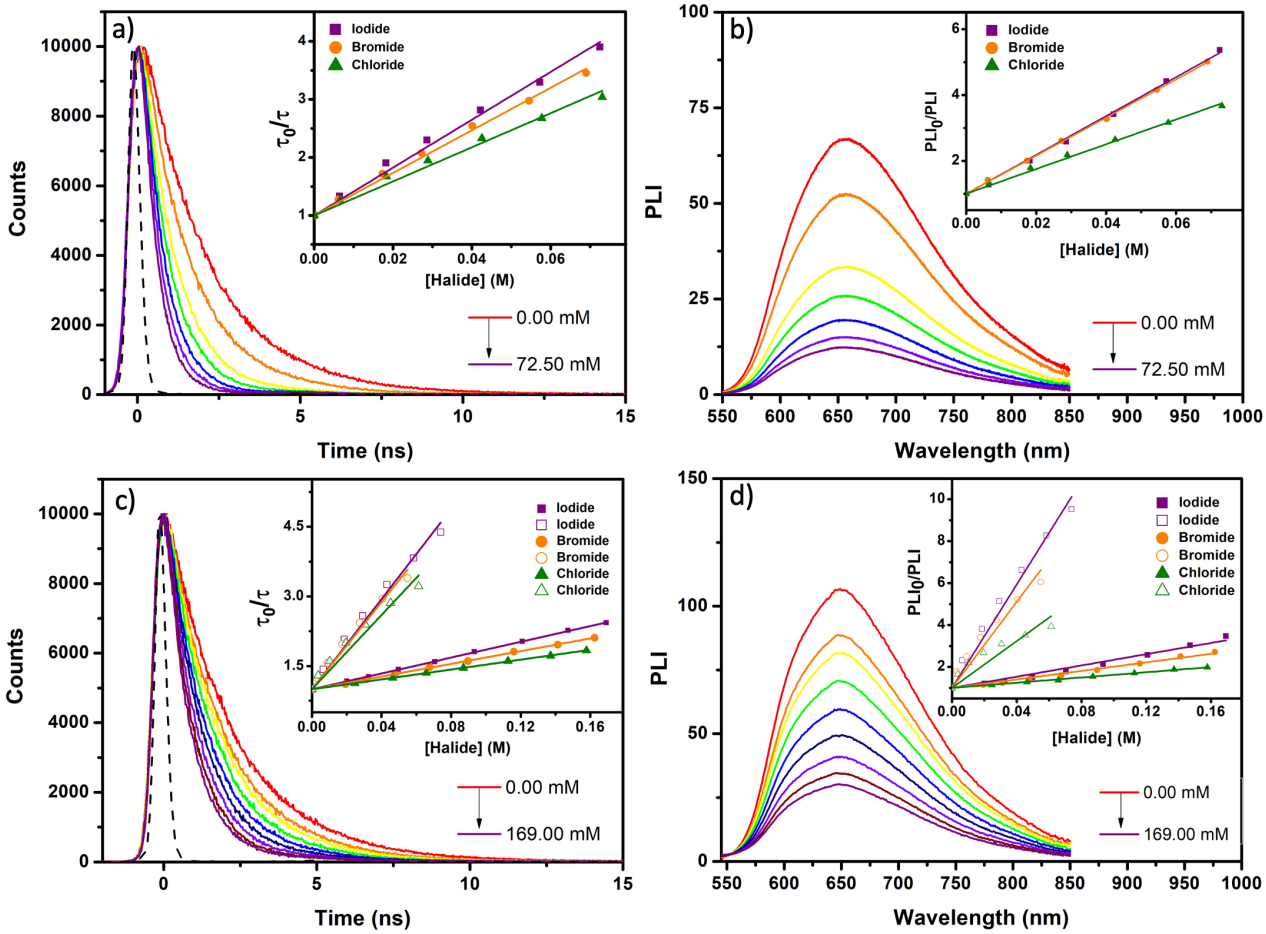

Figure 3. Time-resolved (a,c) and steady-state (b,d) excited-state quenching of $[Fe(phtmeimb)_2]^+$ with iodide in argon purged CH_3CN (a, b) and in CH_2Cl_2 with 0.5 M $TBAPF_6$ (c,d). The inset represents the corresponding Stern-Volmer plots with iodide (purple), bromide (orange) and chloride (green) in CH_3CN (a,b) and in CH_2Cl_2 (c,d, open symbols) and CH_2Cl_2 containing 0.5 M $TBAPF_6$ (c, d, closed symbols).

As Stern-Volmer experiments do not inform on the exact nature of the quenching process, nanosecond transient absorption spectroscopy was carried out to gain insight into the mechanism of the photo-induced process.[58] Pulsed 470 nm light excitation of solutions containing $[Fe(phtmeimb)_2]^+$ and iodide showed clear evidence for excited-state electron transfer in CH_2Cl_2 and CH_3CN (**Figure 4** and **Figures S13-16**). This was evidence by novel absorption features centered at 385 nm and 750 nm, attributed to a combination of a reduced $[Fe(phtmeimb)_2]$ species and $I_2^{\bullet-}$, the latter formed through a reaction between $I^\bullet$ and I^-.[59-63] The kinetic rate constant for the formation of $I_2^{\bullet-}$ could not be determined as it appeared within the instrument's response. Modelling of the transient absorption spectra using authentic spectra of the reduced photosensitizer and $I_2^{\bullet-}$ highlighted that they were formed in a 1:1 ratio (**Figure 4 and Figure S19**). Direct evidence for excited-state electron transfer was not observed with the other halides or in CH_3CN/H_2O 1:1 (**Figures S17-S18**).

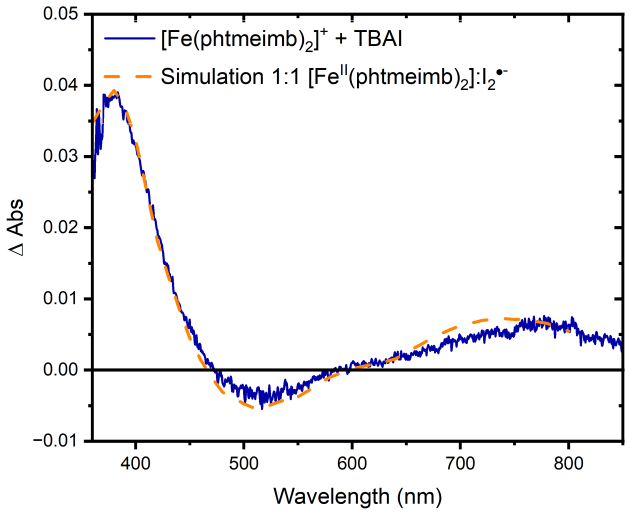

Figure 4. Nanosecond transient absorption spectrum (blue) of a solution containing $[Fe(phtmeimb)_2]^+$ and 45 mM of iodide in CH_2Cl_2. Spectrum is shown 25 ns after the laser pulse and was integrated for 50 ns. The spectra were modeled (orange dashed line) using a 1:1 ratio of Fe(II) to $I_2^{\bullet-}$ (2.45 µM of each). Experiments were carried out in argon purged solvents using 470 nm pulsed light excitation at 10 mJ/pulse.

The cage-escape yields (Φ_{CE}), i.e. the efficiency with which the geminate pair of radicals separate after bimolecular excited-state electron transfer were quantified by comparative actinometry using **Eq. 1** and **2** with $[Ru(bpy)_3]^{2+}$ as actinometer.[64]

$$\Phi_{CE} = \frac{\Phi}{\%\, PL\ Quenched} \qquad \text{Eq. 1}$$

$$\Phi = \left(\frac{\frac{\Delta A_{PS^-}}{\Delta \varepsilon_{PS^-}}}{\frac{\Delta A_{ES_{ref}}}{\Delta \varepsilon_{ES_{ref}}}} \right) \left(\frac{1-10^{-Abs_{ref}(\lambda exc)}}{1-10^{-Abs_{PS}(\lambda exc)}} \right) \qquad \text{Eq. 2}$$

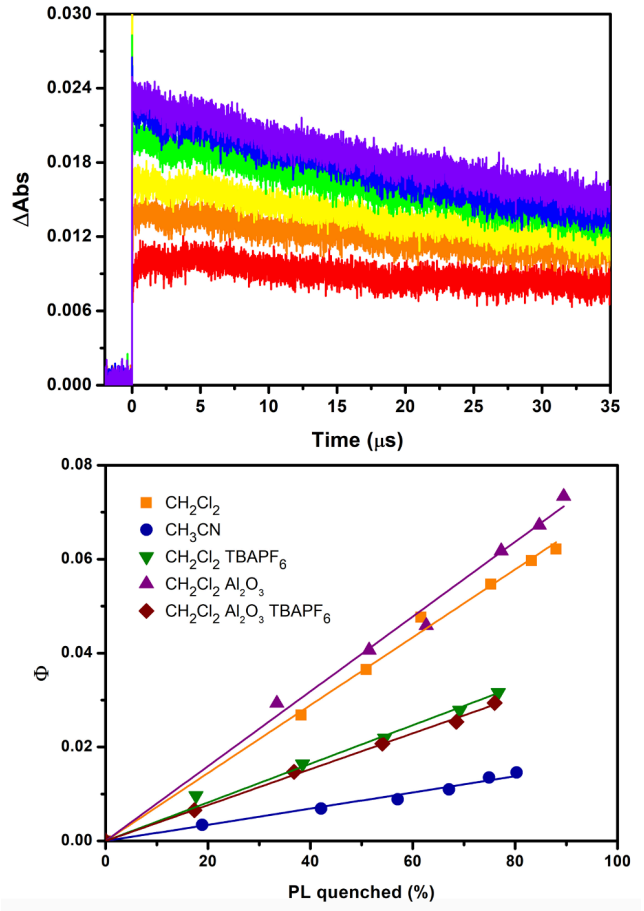

Figure 5. Single wavelength absorption changes recorded at 385 nm following pulsed light 470 nm excitation in the presence of increasing amounts of iodide (top). The single wavelength absorption changes were deconvoluted using a 1:1 ratio of reduced [Fe(phtmeimb)$_2$] to $I_2^{\bullet-}$ which was used to determine the cage-escape yields (bottom).

The transient absorption changes were monitored at 385 nm, i.e. at the maximum absorption changes corresponding to a combination of the reduced photosensitizer and $I_2^{\bullet-}$ (**Figure 5**). As spectral modelling showed that these were produced in a 1:1 ratio (**Figure 4**), the single wavelength absorption changes were analyzed using $\Delta\varepsilon_{385nm}$ = 7200 $M^{-1}cm^{-1}$ and 8600 $M^{-1}cm^{-1}$ for Fe(II) and $I_2^{\bullet-}$, respectively.[23, 40] These signals were compared to the changes in absorption of the reference $[Ru(bpy)_3]^{2+}$ (ES_{ref}) at 450nm. A $\Delta\varepsilon$ value of –11000 $M^{-1}cm^{-1}$ was used for the actinometer at 450 nm.[65-67] Φ_{CE} were obtained by comparing the relative yield of mono-reduced PS produced (Φ) to the percentage of quenched photoluminescence (%PL). Using this procedure, cage-escape yields ranged from 0.079 in dichloromethane to 0.017 in acetonitrile (**Table 2**). Φ_{CE} could not be determined for bromide and chloride. This could imply that the in-cage geminate charge recombination is much faster than the cage-escape process.[41] These Φ_{CE} are small compared to values recorded in organic solvents for photosensitizers where $X_2^{\bullet-}$ was observed, with values of 0.25-0.96.[34, 60, 68] In some instances, low Φ_{CE} (~0.04) with observation of $I_2^{\bullet-}$ in acetonitrile have also been reported using Ru(II) photosensitizers.[62]

Table 2. Cage-escape yields for the reaction between $[Fe(phtmeimb)_2]^+$ and iodide in the indicated solvent.

Solvent	Φ_{CE}
CH_3CN	0.017
CH_2Cl_2	0.072
CH_2Cl_2 – Al_2O_3	0.079
CH_2Cl_2 – 0.5 M $TBAPF_6$	0.041
CH_2Cl_2 – Al_2O_3 – 0.5 M $TBAPF_6$	0.038

The origin of the difference in Φ_{CE} is at this stage not easy to rationalize. Contrary to what has been reported in the literature, there does not seem to be any effect of the driving force for geminate charge recombination on the Φ_{CE}, as larger Φ_{CE} would have otherwise been observed with bromide and chloride.[69-76] An impact of the solvent on the intersystem crossing of the geminate radical pair, as previously hypothesized,[45] may result in state mixing with a higher spin state such as the ^{4}CS which would convey a partial spin-forbidden character to geminate charge recombination, thus increasing Φ_{CE}. Iodide could also promote such state mixing through heavy atom effect compared to the other halides, hence increasing the spin-forbidden character of the geminate charge recombination. Excited-state electron transfer would yield an overall neutral reduced photosensitizer and a neutral halogen atom and as such, electrostatic repulsion is not expected to be a main contributor to these Φ_{CE}, although the data in CH_2Cl_2 and with added electrolyte could suggest otherwise. As iodide is the most polarizable halide, we propose that the larger Φ_{CE} observed in dichloromethane stems from either a better solvation of the separated iodine atom and the reduced photosensitizer than in acetonitrile or that the geminate radical pair is more stabilized in acetonitrile, decreasing the gap with the ground state product, thus favoring recombination.

In conclusions, a known Fe(III) photosensitizer was used for bimolecular excited-state reactivity with iodide, bromide and chloride in CH_2Cl_2, CH_3CN and CH_3CN/H_2O 1:1 mixture. Steady-state and time-resolved excited-state quenching experiments were in line with dynamic quenching with a potentially small static quenching process. Large quenching rate constant were obtained in most conditions. Unambiguous proof for excited-state electron transfer was obtained with iodide, where both the monoreduced photosensitizer and $I_2^{\bullet-}$ were spectroscopically observed. The absence of signals for bromide and chloride suggests that the in-cage geminate charge recombination is faster than the kinetics for the cage-escape process.[41] Φ_{CE} for the reaction with iodide were determined and ranged from 0.079 to 0.017 in CH_2Cl_2 and CH_3CN, respectively. The origin of the difference in Φ_{CE} is currently under investigation. These results however highlight the great versatility of $[Fe(phtmeimb)_2]^+$ since its initial report by Wärnmark and co-workers in 2019 and open great opportunity for bimolecular excited-state reactivity of iron complexes in photoredox catalysis and solar fuels formation.

ASSOCIATED CONTENT

Supporting Information

Additional experimental details, Stern-Volmer experiments, and additional transient absorption spectra and cage-escape yields measurements. The Supporting Information is available free of charge on the ACS Publications website.

AUTHOR INFORMATION

Corresponding Author

Ludovic.Troian@uclouvain.be
Benjamin.Elias@uclouvain.be

Author Contributions

The manuscript was written through contributions of all authors. All authors have given approval to the final version of the manuscript.

Funding Sources

Grant no. 23/28-135 (L.T.-G and B.E.).
Grant no. U.N021.21 (B.E.).
Grant no. 40020332 (L.T.-G).

ACKNOWLEDGMENT

This work was supported by the "Action de Recherche Concertée" through the project "UNCAGED" under grant no. 23/28-135. This work was supported by the Fonds de la Recherche Scientifique (F.R.S.-FNRS) under grant n° U.N021.21 (B.E.) and grant CDR n°40020332. L.T.-G. is a Chercheur Qualifié of the Fonds de la Recherche Scientifique – FNRS. A. R. thanks the Belgian National Funds for Scientific Research (F.R.S.-FNRS) for their Fund for Research Training in Industry and Agriculture (FRIA) PhD grant. S. D. K., A.R., B.E. and L.T.-G. gratefully acknowledge the UCLouvain for financial support.

REFERENCES

1. Segev, G.; Kibsgaard, J.; Hahn, C.; Xu, Z. J.; Cheng, W.-H.; Deutsch, T. G.; Xiang, C.; Zhang, J. Z.; Hammarström, L.; Nocera, D. G.*, et al.*, The 2022 Solar Fuels Roadmap. *J. Phys. D Appl. Phys.* **2022,** *55*, 323003.
2. Nocera, D. G., The Artificial Leaf. *Acc. Chem. Res.* **2012,** *45*, 767-776.
3. Thorarinsdottir, A. E.; Veroneau, S. S.; Nocera, D. G., Self-Healing Oxygen Evolution Catalysts. *Nature Comm.* **2022,** *13*, 1243.
4. Feng, C.; Wang, F.; Liu, Z.; Nakabayashi, M.; Xiao, Y.; Zeng, Q.; Fu, J.; Wu, Q.; Cui, C.; Han, Y.*, et al.*, A Self-Healing Catalyst for Electrocatalytic and Photoelectrochemical Oxygen Evolution in Highly Alkaline Conditions. *Nature Comm.* **2021,** *12*, 5980.
5. Maeda, K.; Teramura, K.; Lu, D.; Takata, T.; Saito, N.; Inoue, Y.; Domen, K., Photocatalyst Releasing Hydrogen from Water. *Nature* **2006,** *440*, 295-295.
6. Wang, Q.; Domen, K., Particulate Photocatalysts for Light-Driven Water Splitting: Mechanisms, Challenges, and Design Strategies. *Chem. Rev.* **2020,** *120*, 919-985.
7. Pornrungroj, C.; Mohamad Annuar, A. B.; Wang, Q.; Rahaman, M.; Bhattacharjee, S.; Andrei, V.; Reisner, E., Hybrid Photothermal–Photocatalyst Sheets for Solar-Driven Overall Water Splitting Coupled to Water Purification. *Nat. Water* **2023,** *1*, 952-960.
8. Rahaman, M.; Andrei, V.; Wright, D.; Lam, E.; Pornrungroj, C.; Bhattacharjee, S.; Pichler, C. M.; Greer, H. F.; Baumberg, J. J.; Reisner, E., Solar-Driven Liquid Multi-Carbon Fuel Production Using a Standalone Perovskite–Bivo4 Artificial Leaf. *Nat. Energy* **2023,** *8*, 629-638.
9. Andrei, V.; Wang, Q.; Uekert, T.; Bhattacharjee, S.; Reisner, E., Solar Panel Technologies for Light-to-Chemical Conversion. *Acc. Chem. Res.* **2022,** *55*, 3376-3386.
10. Andrei, V.; Ucoski, G. M.; Pornrungroj, C.; Uswachoke, C.; Wang, Q.; Achilleos, D. S.; Kasap, H.; Sokol, K. P.; Jagt, R. A.; Lu, H.*, et al.*, Floating Perovskite-Bivo4 Devices for Scalable Solar Fuel Production. *Nature* **2022,** *608*, 518-522.
11. Shan, B.; Vanka, S.; Li, T.-T.; Troian-Gautier, L.; Brennaman, M. K.; Mi, Z.; Meyer, T. J., Binary Molecular-Semiconductor P–N Junctions for Photoelectrocatalytic Co2 Reduction. *Nat. Energy* **2019,** *4*, 290-299.
12. Shan, B.; Brennaman, M. K.; Troian-Gautier, L.; Liu, Y.; Nayak, A.; Klug, C. M.; Li, T.-T.; Bullock, R. M.; Meyer, T. J., A Silicon-Based Heterojunction Integrated with a Molecular Excited State in a Water-Splitting Tandem Cell. *J. Am. Chem. Soc.* **2019,** *141*, 10390-10398.
13. Andreiadis, E. S.; Chavarot-Kerlidou, M.; Fontecave, M.; Artero, V., Artificial Photosynthesis: From Molecular Catalysts for Light-Driven Water Splitting to Photoelectrochemical Cells. *Photochem. Photobiol.* **2011,** *87*, 946-964.
14. Artero, V.; Chavarot-Kerlidou, M.; Fontecave, M., Splitting Water with Cobalt. *Angew. Chem. Int. Ed.* **2011,** *50*, 7238-7266.
15. Windle, C. D.; Kumagai, H.; Higashi, M.; Brisse, R.; Bold, S.; Jousselme, B.; Chavarot-Kerlidou, M.; Maeda, K.; Abe, R.; Ishitani, O.; Artero, V., Earth-Abundant Molecular Z-Scheme Photoelectrochemical Cell for Overall Water-Splitting. *J. Am. Chem. Soc.* **2019,** *141*, 9593-9602.
16. Brennaman, M. K.; Dillon, R. J.; Alibabaei, L.; Gish, M. K.; Dares, C. J.; Ashford, D. L.; House, R. L.; Meyer, G. J.; Papanikolas, J. M.; Meyer, T. J., Finding the Way to Solar Fuels with Dye-Sensitized Photoelectrosynthesis Cells. *J. Am. Chem. Soc.* **2016,** *138*, 13085-13102.
17. Abraham, K. M., Prospects and Limits of Energy Storage in Batteries. *J. Phys. Chem. Lett.* **2015,** *6*, 830-844.
18. Wang, Q.; Pornrungroj, C.; Linley, S.; Reisner, E., Strategies to Improve Light Utilization in Solar Fuel Synthesis. *Nat. Energy* **2022,** *7*, 13-24.
19. Spitler, M. T.; Modestino, M. A.; Deutsch, T. G.; Xiang, C. X.; Durrant, J. R.; Esposito, D. V.; Haussener, S.; Maldonado, S.; Sharp, I. D.; Parkinson, B. A.*, et al.*, Practical Challenges in the Development of Photoelectrochemical Solar Fuels Production. *Sustainable Energy Fuels* **2020,** *4*, 985-995.
20. Dogutan, D. K.; Nocera, D. G., Artificial Photosynthesis at Efficiencies Greatly Exceeding That of Natural Photosynthesis. *Acc. Chem. Res.* **2019,** *52*, 3143-3148.
21. Bold, S.; Massin, J.; Giannoudis, E.; Koepf, M.; Artero, V.; Dietzek, B.; Chavarot-Kerlidou, M., Spectroscopic Investigations Provide a Rationale for the Hydrogen-Evolving Activity of Dye-Sensitized Photocathodes Based on a Cobalt Tetraazamacrocyclic Catalyst. *ACS Catal.* **2021,** *11*, 3662-3678.
22. Sampaio, R. N.; Troian-Gautier, L.; Meyer, G. J., A Charge-Separated State That Lives for Almost a Second at a Conductive Metal Oxide Interface. *Angew. Chem.* **2018,** *130*, 15616-15620.
23. Troian-Gautier, L.; Turlington, M. D.; Wehlin, S. A. M.; Maurer, A. B.; Brady, M. D.; Swords, W. B.; Meyer, G. J., Halide Photoredox Chemistry. *Chem. Rev.* **2019,** *119*, 4628-4683.
24. Hu, K.; Sampaio, R. N.; Schneider, J.; Troian-Gautier, L.; Meyer, G. J., Perspectives on Dye Sensitization of Nanocrystalline Mesoporous Thin Films. *J. Am. Chem. Soc.* **2020,** *142*, 16099-16116.
25. De Kreijger, S.; Schott, O.; Troian-Gautier, L.; Cauët, E.; Hanan, G. S.; Elias, B., Red Absorbing Cyclometalated Ir(Iii) Diimine Photosensitizers Competent for Hydrogen Photocatalysis. *Inorg. Chem.* **2022,** *61*, 5245-5254.
26. Cotic, A.; Cerfontaine, S.; Slep, L. D.; Elias, B.; Troian-Gautier, L.; Cadranel, A., Anti-Dissipative Strategies toward More Efficient Solar Energy Conversion. *J. Am. Chem. Soc.* **2023,** *145*, 5163-5173.
27. Bolton, J. R., Solar Photoproduction of Hydrogen: A Review. *Sol. Energy* **1996,** *57*, 37-50.
28. Shang, B.; Rooney, C. L.; Gallagher, D. J.; Wang, B. T.; Krayev, A.; Shema, H.; Leitner, O.; Harmon, N. J.; Xiao, L.; Sheehan,

C.*, et al.*, Aqueous Photoelectrochemical Co2 Reduction to Co and Methanol over a Silicon Photocathode Functionalized with a Cobalt Phthalocyanine Molecular Catalyst. *Angew. Chem. Int. Ed.* **2023,** *62*, e202215213.

29. Müller, A. V.; Ahmad, S.; Sirlin, J. T.; Ertem, M. Z.; Polyansky, D. E.; Grills, D. C.; Meyer, G. J.; Sampaio, R. N.; Concepcion, J. J., Reduction of Co to Methanol with Recyclable Organic Hydrides. *J. Am. Chem. Soc.* **2024**. https://doi.org/10.1021/jacs.3c14605

30. Brady, M. D.; Sampaio, R. N.; Wang, D.; Meyer, T. J.; Meyer, G. J., Dye-Sensitized Hydrobromic Acid Splitting for Hydrogen Solar Fuel Production. *Journal of the American Chemical Society* **2017,** *139*, 15612-15615.

31. Brady, M. D.; Troian-Gautier, L.; Sampaio, R. N.; Motley, T. C.; Meyer, G. J., Optimization of Photocatalyst Excited- and Ground-State Reduction Potentials for Dye-Sensitized Hbr Splitting. *ACS Appl. Mater. Interfaces* **2018,** *10*, 31312-31323.

32. Bevernaegie, R.; Wehlin, S. A. M.; Piechota, E. J.; Abraham, M.; Philouze, C.; Meyer, G. J.; Elias, B.; Troian-Gautier, L., Improved Visible Light Absorption of Potent Iridium(Iii) Photo-Oxidants for Excited-State Electron Transfer Chemistry. *J. Am. Chem. Soc.* **2020,** *142*, 2732-2737.

33. Deetz, A. M.; Troian-Gautier, L.; Wehlin, S. A. M.; Piechota, E. J.; Meyer, G. J., On the Determination of Halogen Atom Reduction Potentials with Photoredox Catalysts. *J. Phys. Chem. A* **2021,** *125*, 9355-9367.

34. De Kreijger, S.; Elias, B.; Troian-Gautier, L., Chloride, Bromide, and Iodide Photooxidation in Acetonitrile/Water Mixtures Using Binuclear Iridium(Iii) Photosensitizers. *Inorg. Chem.* **2023,** *62*, 16196-16202.

35. Li, G.; Ward, W. M.; Meyer, G. J., Visible Light Driven Nanosecond Bromide Oxidation by a Ru Complex with Subsequent Br–Br Bond Formation. *J. Am. Chem. Soc.* **2015,** *137*, 8321-8323.

36. Li, G.; Swords, W. B.; Meyer, G. J., Bromide Photo-Oxidation Sensitized to Visible Light in Consecutive Ion Pairs. *J. Am. Chem. Soc.* **2017,** *139*, 14983-14991.

37. Wehlin, S. A. M.; Troian-Gautier, L.; Li, G.; Meyer, G. J., Chloride Oxidation by Ruthenium Excited-States in Solution. *J. Am. Chem. Soc.* **2017,** *139*, 12903-12906.

38. Li, P.; Deetz, A. M.; Hu, J.; Meyer, G. J.; Hu, K., Chloride Oxidation by One- or Two-Photon Excitation of N-Phenylphenothiazine. *J. Am. Chem. Soc.* **2022,** *144*, 17604-17610.

39. Schwarz, J.; Ilic, A.; Johnson, C.; Lomoth, R.; Wärnmark, K., High Turnover Photocatalytic Hydrogen Formation with an Fe(Iii) N-Heterocyclic Carbene Photosensitiser. *Chem. Commun.* **2022,** *58*, 5351-5354.

40. Kjær, K. S.; Kaul, N.; Prakash, O.; Chábera, P.; Rosemann, N. W.; Honarfar, A.; Gordivska, O.; Fredin, L. A.; Bergquist, K.-E.; Häggström, L*., et al.*, Luminescence and Reactivity of a Charge-Transfer Excited Iron Complex with Nanosecond Lifetime. *Science* **2019,** *363*, 249-253.

41. Rosemann, N. W.; Chábera, P.; Prakash, O.; Kaufhold, S.; Wärnmark, K.; Yartsev, A.; Persson, P., Tracing the Full Bimolecular Photocycle of Iron(Iii)–Carbene Light Harvesters in Electron-Donating Solvents. *J. Am. Chem. Soc.* **2020,** *142*, 8565-8569.

42. Prakash, O.; Lindh, L.; Kaul, N.; Rosemann, N. W.; Losada, I. B.; Johnson, C.; Chábera, P.; Ilic, A.; Schwarz, J.; Gupta, A. K*., et al.*, Photophysical Integrity of the Iron(Iii) Scorpionate Framework in Iron(Iii)–Nhc Complexes with Long-Lived 2lmct Excited States. *Inorg. Chem.* **2022**.

43. de Groot, L. H. M.; Ilic, A.; Schwarz, J.; Wärnmark, K., Iron Photoredox Catalysis–Past, Present, and Future. *J. Am. Chem. Soc.* **2023,** *145*, 9369-9388.

44. Rosemann, N. W.; Lindh, L.; Bolaño Losada, I.; Kaufhold, S.; Prakash, O.; Ilic, A.; Schwarz, J.; Wärnmark, K.; Chábera, P.; Yartsev, A.; Persson, P., Competing Dynamics of Intramolecular Deactivation and Bimolecular Charge Transfer Processes in Luminescent Fe(Iii) N-Heterocyclic Carbene Complexes. *Chem. Sci.* **2023,** *14*, 3569-3579.

45. Aydogan, A.; Bangle, R. E.; Cadranel, A.; Turlington, M. D.; Conroy, D. T.; Cauët, E.; Singleton, M. L.; Meyer, G. J.; Sampaio, R. N.; Elias, B.; Troian-Gautier, L., Accessing Photoredox Transformations with an Iron(Iii) Photosensitizer and Green Light. *J. Am. Chem. Soc.* **2021,** *143*, 15661-15673.

46. Aydogan, A.; Bangle, R. E.; De Kreijger, S.; Dickenson, J. C.; Singleton, M. L.; Cauët, E.; Cadranel, A.; Meyer, G. J.; Elias, B.; Sampaio, R. N.; Troian-Gautier, L., Mechanistic Investigation of a Visible Light Mediated Dehalogenation/Cyclisation Reaction Using Iron(Iii), Iridium(Iii) and Ruthenium(Ii) Photosensitizers. *Catal. Sci. Technol.* **2021,** *11*, 8037-8051.

47. Glaser, F.; Aydogan, A.; Elias, B.; Troian-Gautier, L., The Great Strides of Iron Photosensitizers for Contemporary Organic Photoredox Catalysis: On Our Way to the Holy Grail? *Coord. Chem. Rev.* **2024,** *500*, 215522.

48. Ripak, A.; De Kreijger, S.; Sampaio, R. N.; Vincent, C. A.; Cauët, É.; Jabin, I.; Tambar, U. K.; Elias, B.; Troian-Gautier, L., Photosensitized Activation of Diazonium Derivatives for C–B Bond Formation. *Chem Catal.* **2023**, 100490.

49. Kaul, N.; Lomoth, R., The Carbene Cannibal: Photoinduced Symmetry-Breaking Charge Separation in an Fe(Iii) N-Heterocyclic Carbene. *J. Am. Chem. Soc.* **2021,** *143*, 10816-10821.

50. Note that the slope determined from the steady-state photoluminescence data (PLI_0/PLI) was systematically slightly larger than the one determined from the time-resolved data (τ_0/τ). This could be indicative of a small static quenching contribution. Static constant of 2.32, 1.78 and 0.55 M^{-1} were determined for iodide, bromide and chloride, respectively, in dichloromethane containing 0.5M $TBAPF_6$.

51. Verity, B.; Bigger, S. W., The Dependence of Quinine Fluorescence Quenching on Ionic Strength. *Int. J. Chem. Kinet.* **1996,** *28*, 919-923.

52. Glaser, F.; Schmitz, M.; Kerzig, C., Coulomb Interactions for Mediator-Enhanced Sensitized Triplet–Triplet Annihilation Upconversion in Solution. *Nanoscale* **2024,** *16*, 123-137.

53. Bronsted, J. N.; Teeter, C. E., On Kinetic Salt Effect. *J. Phys. Chem* **1924,** *28*, 579-587.

54. Jonnalagadda, S. B.; Gollapalli, N. R., Kinetics of Reduction of Toluidine Blue with Sulfite—Kinetic Salt Effect in Elucidation of Mechanism. *J. Chem. Ed.* **2000,** *77*, 506.

55. Indelli, A., Kinetic Salt Effects by the Tetraalkylammonium Ions. *J. Phys. Chem* **1961,** *65*, 972-974.

56. McTigue, P. T., Theory of Kinetic Salt Effects. *Trans. Faraday Soc.* **1964,** *60*, 127-136.

57. Armarego, W. L. F., Chapter 4 - Purification of Inorganic and Metal-Organic Chemicals. In *Purification of Laboratory Chemicals (Eighth Edition)*, Armarego, W. L. F., Ed. Butterworth-Heinemann: 2017; pp 635-770.

58. De Kreijger, S.; Gillard, M.; Elias, B.; Troian-Gautier, L., Spectroscopic Techniques to Unravel Mechanistic Details in Light-Induced Transformations and Photoredox Catalysis. *ChemCatChem* **2024,** *16*, e202301100.

59. Clark, C. C.; Marton, A.; Meyer, G. J., Evidence for Static Quenching of Mlct Excited States by Iodide. *Inorg. Chem.* **2005,** *44*, 3383-3385.

60. Marton, A.; Clark, C. C.; Srinivasan, R.; Freundlich, R. E.; Narducci Sarjeant, A. A.; Meyer, G. J., Static and Dynamic Quenching of Ru(Ii) Polypyridyl Excited States by Iodide. *Inorg. Chem.* **2006,** *45*, 362-369.

61. Gardner, J. M.; Giaimuccio, J. M.; Meyer, G. J., Evidence for Iodine Atoms as Intermediates in the Dye Sensitized Formation of I−I Bonds. *J. Am. Chem. Soc.* **2008,** *130*, 17252-17253.

62. Gardner, J. M.; Abrahamsson, M.; Farnum, B. H.; Meyer, G. J., Visible Light Generation of Iodine Atoms and I−I Bonds: Sensitized I− Oxidation and I_3^- Photodissociation. *J. Am. Chem. Soc.* **2009,** *131*, 16206-16214.

63. Troian-Gautier, L.; Swords, W. B.; Meyer, G. J., Iodide Photoredox and Bond Formation Chemistry. *Acc. Chem. Res.* **2019,** *52*, 170-179.

64. Ripak, A.; De Kreijger, S.; Elias, B.; Troian-Gautier, L., A Protocol for Determining Cage-Escape Yields Using Nanosecond Transient Absorption Spectroscopy. *STAR Protocols* **2023,** *4*, 102312.

65. Yoshimura, A.; Hoffman, M. Z.; Sun, H., An Evaluation of the Excited State Absorption Spectrum of Ru(Bpy)32+ in Aqueous and Acetonitrile Solutions. *J. Photoch. Photobio. A* **1993,** *70*, 29-33.

66. Goez, M.; von Ramin-Marro, D.; Othman Musa, M. H.; Schiewek, M., Photoionization of [Ru(Bpy)3]2+: A Catalytic Cycle with Water as Sacrificial Donor. *J. Phys. Chem. A* **2004,** *108*, 1090-1100.

67. Müller, P.; Brettel, K., [Ru(Bpy)3]2+ as a Reference in Transient Absorption Spectroscopy: Differential Absorption Coefficients for Formation of the Long-Lived 3mlct Excited State. *Photochem. Photobio. Sci.* **2012,** *11*, 632-636.

68. Troian-Gautier, L.; Beauvilliers, E. E.; Swords, W. B.; Meyer, G. J., Redox Active Ion-Paired Excited States Undergo Dynamic Electron Transfer. *J. Am. Chem. Soc.* **2016,** *138*, 16815-16826.

69. Wang, C.; Li, H.; Bürgin, T. H.; Wenger, O. S., Cage Escape Governs Photoredox Reaction Rates and Quantum Yields. *Nature Chem.* **2024**. https://doi.org/10.1038/s41557-024-01482-4

70. Ohno, T.; Yoshimura, A.; Mataga, N., Bell-Shaped Energy-Gap Dependence of Backward Electron Transfer Occurring within Geminate Radical Pairs Produced by Quenching of Ruthenium(Ii) Polypyridine Complexes by Aromatic Amines. *J. Phys. Chem* **1990,** *94*, 4871-4876.

71. Gould, I. R.; Ege, D.; Moser, J. E.; Farid, S., Efficiencies of Photoinduced Electron-Transfer Reactions: Role of the Marcus Inverted Region in Return Electron Transfer within Geminate Radical-Ion Pairs. *J. Am. Chem. Soc.* **1990,** *112*, 4290-4301.

72. Burget, D.; Jacques, P.; Vauthey, E.; Suppan, P.; Haselbach, E., Marcus Inverted Region: Nature of Donor–Acceptor Pairs and Free Ion Yields. *J. Chem. Soc., Faraday Trans.* **1994,** *90*, 2481-2487.

73. Niwa, T.; Kikuchi, K.; Matsusita, N.; Hayashi, M.; Katagiri, T.; Takahashi, Y.; Miyashi, T., Solvent Effects on Photoinduced Electron-Transfer Reactions. *J. Phys. Chem* **1993,** *97*, 11960-11964.

74. Kikuchi, K.; Niwa, T.; Takahashi, Y.; Ikeda, H.; Miyashi, T., Quenching Mechanism in a Highly Exothermic Region of the Rehm-Weller Relationship for Electron-Transfer Fluorescence Quenching. *J. Phys. Chem* **1993,** *97*, 5070-5073.

75. Hino, T.; Akazawa, H.; Masuhara, H.; Mataga, N., Ionic Photodissociation of Excited Electron Donor-Acceptor Systems. Ii. Importance of the Chemical Property of Donor-Acceptor Pairs. *J. Phys. Chem* **1976,** *80*, 33-37.

76. Zanini, G. P.; Montejano, H. A.; Previtali, C. M., Photoinduced Electron-Transfer Quenching of Excited Singlet States of Polycyclic Aromatic Hydrocarbons by Organic Acceptors. *J. Chem. Soc., Faraday Trans.* **1995,** *91*, 1197-1202.

For TOC Use Only

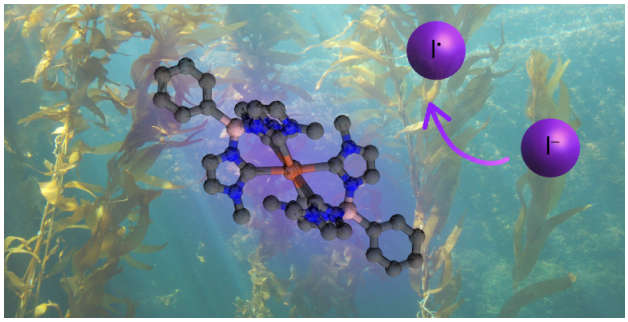

A Fe(III) photosensitizer with ligand-to-metal charge transfer (LMCT) excited state was used to perform visible light halide oxidation of iodide, bromide and chloride in dichloromethane, acetonitrile and acetonitrile/water 1:1 mixtures. A combination of steady-state and time-resolved spectroscopic techniques confirmed that reductive excited-state electron transfer occurred efficiently with iodide. Cage-escape yields were quantified by comparative actinometry and ranged from 0.079 in dichloromethane to 0.017 in acetonitrile.